Arabian Journal of Chemistry 16 (2023) 105315

Contents lists available at ScienceDirect

Arabian Journal of Chemistry

journal homepage: www.sciencedirect.com

Original article

Co-hydrothermally carbonized sewage sludge and lignocellulosic biomass: An efficiently renewable solid fuel

Siridet Piboonudomkarn [a], Pongtanawat Khemthong [b], Saran Youngjan [b], Kitirote Wantala [c], Visanu Tanboonchuy [a], Yingyote Lubphoo [d], Rattabal Khunphonoi [a,e,*]

[a] Department of Environmental Engineering, Khon Kaen University, Khon Kaen 40002, Thailand
[b] National Nanotechnology Center (NANOTEC), National Science and Technology Development Agency (NSTDA), Klong Luang, Pathumthani 12120, Thailand
[c] Department of Chemical Engineering, Faculty of Engineering, Khon Kaen University, Khon Kaen 40002, Thailand
[d] Department of Industrial Piping Technology, Faculty of Technical Education, Rajamangala University of Technology Isan, Khon Kaen Campus, Khon Kaen 40000, Thailand
[e] Research Center for Environmental and Hazardous Substance Management (EHSM), Faculty of Engineering, Khon Kaen University, Khon Kaen 40002, Thailand

ARTICLE INFO

Article history:
Received 15 June 2023
Accepted 26 September 2023
Available online 2 October 2023

Keywords:
Co-hydrothermal carbonization
Hydrochar
Lignocellulosic biomass
Sewage sludge
Solid fuel

ABSTRACT

The objectives of this investigation were to elucidate the potential use of metal oxide-rich sewage sludge obtained from the treated brewery wastewater into a value-added solid fuel via co-hydrothermal carbonization process (co-HTC). Two residue biomass including spent coffee grounds and bagasse were supplied as co-combustion. The effects of sewage sludge and biomass addition on fuel properties were evaluated to optimize the best condition for biocoal-liked production. The chemical composition and mineral phase of solid product were further analyzed. Combustion kinetics analysis including activation energy (E) and pre-exponential factor (A) were derived from thermogravimetric analysis. It was found that the addition of coffee grounds and bagasse enhanced the fuel properties of the solid products, remarkably increasing high heating value (HHV) along with a low ash content, providing an increased fuel ratio of 0.34 – 1.01 and higher HHV as 14.29 – 22.19 MJ/kg. The highest rate of energy recovery was achieved when combining 75 wt% sewage sludge with 25 wt% spent coffee grounds. A substantial decrease of H/C and O/C atomic ratios was distinguished after bagasse addition compared to commercial lignite coal. It was also noticed that the relationship between the sewage sludge and biomass feedstocks during co-HTC is synergistic by increasing the amount of oxidative carbon during the char combustion stage and enhancing the degree of thermal stability. Moreover, it was also emphasized that during co-HTC some carbon and inorganic contents of sludge and lignocellulosic biomass were partially transferred into a liquid phase confirmed by TOC and ICP-OES analyses. A heavy metal leaching toxicity in a liquid product was also determined according to the USA-EPA standard. The combustion reactivity was improved, especially combustion reactivity of the biomass-sewage sludge-derived hydrochar. Interestingly, the hydrochar product was anticipated to possess enhanced safety and stability. Moreover, the co-combustion of hydrochar and coal improved the devolatilization properties and ignition of coal. This strategy revealed that co-hydrothermal process with biomass is a prospective approach to increase the value-added of sewage sludge feedstock as bicoal-like solid fuel.

1. Introduction

As an industrial effluent treatment byproduct, sewage sludge is gaining significant attention as a sustainable biomass for bio-oil or solid fuel energy production. With the growth of industrialization and urbanization, a large amount of industrial sewage sludge is generated and is typically disposed of via landfill or incineration, which results in secondary pollution and a low rate of energy recovery (Gai et al., 2016). Due to the toxic substances contained in sewage sludge, excess sludge or its improper management leads to serious environmental problems (Yang et al., 2015). The production of one barrel of beer in a brewery produces approximately 1.3–2 barrels of wastewater (Olajire, 2020), based on production and water consumption. When this wastewater is treated, activated sludge is generated. Academics and industry have therefore increasingly focused on developing an appropriate method for han-

* Corresponding author.
E-mail address: rattakh@kku.ac.th (R. Khunphonoi).
Peer review under responsibility of King Saud University.

Production and hosting by Elsevier

https://doi.org/10.1016/j.arabjc.2023.105315
1878-5352/

dling sewage sludge. Due to the characteristics of sewage sludge such as very high moisture content, pathogens, heavy metals, and high ash content, it is challenging to recycle sewage sludge as a source of renewable energy (Peng et al., 2018).

Hydrothermal carbonization (HTC) is a wet thermochemical process capable of converting sewage sludge into solid fuel (hydrochar) under a facile temperature and autogenously generated pressure (Koottatep et al., 2016; Sattasathuchana et al., 2023). This technique shows good potential for completely sterilizing sludge residue and producing hydrochar. One of the main advantages of HTC is the suitability for biomass materials with a high moisture content, such as sewage sludge, because of its ability to utilize biomass feedstock without drying treatment. The solid:liquid ratio, reaction time, and temperature influence the properties of biochar prepared by treating sludge with HTC (Paiboonudomkarn et al., 2023; Mumme et al., 2015). Temperature is an important parameter in the HTC process because it predominantly affects the properties of the water, contributing to ionic reactions in the subcritical region. At lower temperatures, carbonization produces a greater quantity of solid products. At higher temperatures, carbonization is more intense, leading to the formation of more liquid and gaseous products and fewer solid products (Khoo et al., 2020). In addition, the oxygen and hydrogen concentrations decrease with increasing temperature, indicating the removal of these elements. In contrast, the carbon value has been observed to increase with increasing temperature. However, due to its high ash content, low carbon content, and low heat value after the HTC process, the properties and combustion behavior of hydrochar obtained from sewage sludge indicate that it is not suitable for use as a solid fuel (Lin et al., 2015; Ma et al., 2019; Zheng et al., 2019).

In order to improve the fuel properties of sewage sludge-derived hydrochar, the co-hydrothermal carbonization (co-HTC) of sewage sludge with other solid waste has attracted attention (Bardhan et al., 2021). Lu et al. (2021) conducted the co-HTC of sewage sludge with lignocellulosic biomass and found that compared with sewage sludge alone, the high HHV of the obtained hydrochar was enhanced from 6.10 to 13.23 MJ/kg. The blending ratio of the feedstock is a crucial co-HTC factor that affects denitrification, desulfurization, and fuel characteristics (Zhang et al., 2020). The presence of waste biomass mixed with sewage sludge enhances the properties of solid fuel because the abundant cellulose and lignin contained in biomass residue can improve decarboxylation, dehydration, and demethylation processes during co-HTC (Zhai et al., 2017). These studies demonstrate that incorporating lignocellulosic biomass into industrial sewage sludge hydrochar is a promising method for overcoming the barrier to its energy utilization. Agricultural waste bioresources, such as bagasse and spent coffee grounds, were selected as additive materials in this study. Bagasse, the solid fibrous material remaining after sugarcane juice extraction, is the sugar industry's primary waste product. Processing 1,000 tons of sugarcane generates approximately 270–280 tons of bagasse (Martinez-Hernandez et al., 2018). Bagasse is typically composed of hemicellulose, cellulose, and lignin, and it has a low ash content. All of these components can be utilized for energy production (Reza et al., 2016). Coffee grounds were considered as a further additive because the amount of produced spent coffee grounds has been steadily increasing along with the rise in global coffee consumption (Saberian et al., 2021). Spent coffee grounds are produced during the coffee extraction process, causing a number of environmental issues (McNutt and He, 2019). Spent coffee grounds have high organic content, including carbohydrates, proteins, fiber, caffeine, polyphenol, tannins, and pectin, and they have high calorific value (Kim et al., 2017). As a result, spent coffee grounds have been utilized as a renewable feedstock for the production of fuels (Massaya et al., 2021). Moreover, the co-combustion of solid waste with coal is another alternative method for utilizing solid waste. This strategy supports the carbon economy, the energy sector, and the environment (Tong et al., 2019). From an economic standpoint, the potential co-combustion of biomass and coal in thermal power plants is a desirable alternative because it permits the use of current infrastructure that is already supplied with the necessary equipment for gaseous emission control (Cong et al., 2019). Under the right circumstances, it is possible to dispose of sewage sludge by combining it with coal for co-combustion. Coimbra et al., (2016) investigated coal and sewage sludge co-combustion. TGA-DTG analysis revealed that the composition of sludge affected the activation energy.

In this study, the feasibility of converting sewage sludge derived from activated sludge, which was obtained from wastewater treatment in the brewery industry, was carried out by HTC. The effects of reaction parameters on the solid yields, solid-to-liquid ratio, and reaction temperature were investigated. Co-hydrothermal treatments of sludge and biomass waste with varying blending ratios were examined and the characteristics of the obtained hydrochar were examined. The combustion behavior and kinetics of the hydrochar were also evaluated. Additionally, the co-combustion characteristics of commercial coal blended with different amounts of hydrochar from sludge blends were investigated. The migration behavior of the total concentration of heavy metals in the hydrochars during the hydrothermal reaction was also evaluated. This research on mixing sewage sludge from wastewater treatment with lignocellulosic waste, spent coffee grounds, and bagasse offers a potential strategy for enhancing energy utilization and solving the problem of solid waste disposal.

2. Materials and methods

2.1. Materials

Sewage sludge from the wastewater treatment of the brewery industry in Khon Kaen, Thailand was utilized in this work. To ensure the homogeneity of this sewage sludge, it was ground into a fine powder (<1 mm). Spent coffee grounds, bagasse, and sludge were dried for 24 h at 105 °C.

2.2. Co-hydrothermal carbonization (co-HTC) process

HTC was carried out in a 200 mL autoclave reactor coupling with electronic heater. The effects of solid-to-liquid ratio were remarked as 1:1, 1:3, 1:5, and 1:7. While the reaction temperatures were assigned to 200, 210, and 220 °C. Prior to each experiment, a dried sludge was mixed with DI water before introducing to the autoclave reactor. Then, it was flushed with N_2 gas for 15 min to eliminate the excess air inside the autoclave. For HTC step, the reactor was heated up to the desired temperature and held for 5 h. After completing the reaction, the solid and liquid products were separated and collected. The solid was then dried at 105 °C for 24 h (labelled as HTC-S), while the liquid was kept in the fridge. In addition, the as-synthesized solid samples were labelled as HTC-x:y-z, where x:y represents the solid:liquid ratio and z represents the hydrothermal temperature in degrees Celsius. Moreover, the bare hydrochars obtained from pure spent coffee grounds or bagasse without adding sewage sludge were denoted as HTC-C and HTC-B, respectively.

For co-HTC, only the effect of mixing ratio was investigated by fixing the solid-to-liquid ratio as 1:5 at reaction temperature of 220 °C. The desired mixing ratios were 25, 50, and 75 wt%. In addition, the obtained hydrochars were denoted by their mixing ratio and biomass type (S = sludge, C = spent coffee grounds, and B = bagasse). For example, HTC-25%SC referred to the hydrochar derived from 25% sewage sludge mixed with spent coffee grounds.

2.3. Combustion behavior

The combustion behavior and combustion kinetics of each sample was analysis by using thermogravimetric method (TGA, Mettler, Toledo, USA). Mixtures containing 10, 30, and 50 wt% HTC-S blended with commercial coal were applied to investigate the performance of a co-combustion ability. TGA measurement was carried out under air atmospheric from temperature range of 30 – 700 °C with a heating rate of 10 °C/min and flow rate of 30 mL/min. Ignition temperature (T_i), maximum combustion rate temperature (T_m), and burnout temperature (T_b) were determined by using the TG and DTG profiles. The comprehensive combustibility index (S) was also calculated to examine the combustion reactivity of samples (Wang et al., 2012).

$$S = \frac{(dw/dt)_{max}(dw/dt)_{mean}}{T_i^2 T_b} \quad (1)$$

where $(dw/dt)_{max}$ and $(dw/dt)_{mean}$ represent the maximum and mean rates of weight loss (wt%/min), respectively.

The fundamental rate equation calculated in all solid-state heterogeneous phenomena was the Arrhenius equation (Peng et al., 2016).

$$\frac{d\alpha}{dT} = \frac{A}{\beta}\exp(-\frac{E}{RT})(1-\alpha)^n \quad (2)$$

$$\alpha = (m_0 - m_t)/(m_0 - m_f) \quad (3)$$

where E is the activation energy (kJ/mol) of the reaction, A is the pre-exponential factor (min^{-1}) of the reaction, β is the heating rate (10 K/min), R is the universal gas constant (8.314 J/K.mol), T is the absolute temperature (K), α is the sample conversion rate at time t (derived from the TG–DTG graphs). While m_0, m_t, and m_f are corresponding to the initial, instantaneous, and final mass of samples, respectively.

Using the approximation introduced by the Coats–Redfern (CR) method, Equation (2) can be integrated and rearranged as follows (Li et al., 2020):

$$\ln[\int_0^\alpha \frac{d\alpha}{(1-\alpha)^n T^2}] = \ln[\frac{AR}{\beta E}(1-\frac{2RT}{E})] - \frac{E}{RT} \quad (4)$$

The left side of Equation (4) was plotted against 1/T, providing the slope of the straight line as E/R. The value of E can be calculated from the slope, whereas A is derived from the regression line intercept.

Solid fuel combustion is typically characterized by the first-order kinetic model (n = 1) (Lin et al., 2015). Considering the value of 2RT/E, it is close to zero, it can be noted as a constant. Thus, equation (4) can be simplified as follows:

$$\ln[\frac{-In(1-\alpha)}{T^2}] = \ln\frac{AR}{\beta E} - \frac{E}{RT} \ (n = 1) \quad (5)$$

2.4. Analysis method

Elemental compositions (C, H, N, and S) of the sludge and hydrothermally treated biomass were examined using CHNS analyzers (LECO, 628 series, USA). Moisture, ash, and volatile matter (VM) were measured following the ASTM standards D-3173, D-3174, and D-3175, respectively. The difference determined the fixed carbon content (FC). The higher heating value (HHV) was measured by a bomb calorimeter (IKA, C5000, USA). The surface morphologies were analyzed by scanning electron microscopy (SEM, Hitachi S-3000 N, Japan). Fourier-transform infrared spectroscopy (FTIR, Bruker, USA) was performed at 400–4000 cm^{-1}. The metal content in the solid products and solution was determined by inductively coupled plasma–optical emission spectroscopy (ICP-OES, Perkin Elmer, AVIO 200, Waltham, MA, USA). The total organic carbon (TOC) of the process water was analyzed by a TOC analyzer (Analytik Jena, Model: multi N/C 2100 sla, Germany). The inorganic composed of the raw sludge and solid products were analyzed by X-ray fluorescence spectroscopy (XRF, WDXRF, Rigaku ZSX Primus, USA).

3. Results and discussion

3.1. Fuel properties of raw materials and hydrochars

The characteristics of the sludge and prepared hydrochars were studied to investigate the changes in the relevant characteristics of the raw materials, as shown in Table 1. The raw sludge contained 40.84% ash. After HTC treatment, the ash content of the hydrochars rose under all HTC conditions. The temperature had no significant effect on the increase in ash content after HTC was performed. These results are similar to those of Hansen et al. (2022). However, the ash content rose in proportion to the solid-to-liquid ratio at reaction temperature 200 and 210 °C. Inorganic and organic materials can be extracted from biomass and dissolved in process water. If the loss of organic material is greater than the loss of inorganic material, the ash concentration will increase following the HTC reaction (Hansen et al., 2022). This was confirmed by TOC analysis (Supplementary Information, Figure S1), indicating that increasing the solid-to-liquid ratio increased the TOC concentration in the process water. The increased ash content was mainly caused by the decomposition and transformation of organic material during HTC, including dehydration, decarboxylation, hydrolysis, deamination, and gasification (Nanda et al., 2017). After 5 h of hydrothermal treatment, volatile matter (VM) was reduced by hydrolysis (Wang et al., 2019). The solid-to-liquid ratio and reaction temperature affected the yield of hydrochar. The yield of hydrochar notably decreased with increasing solid-to-liquid ratio and reaction temperature. This was in good agreement with Xu et al. (2020). Carbonization is greater at higher temperatures, resulting in the production of more liquid and gaseous products and a reduced solid yield (Tasca et al., 2019). Fixed carbon decreased when the ratio of solid-to-liquid increased. Therefore, a moderate temperature is required to retain the maximum amount of fixed carbon in hydrochar following the HTC of sewage sludge (Danso-Boateng et al., 2015).

The HHV of the hydrochars is presented in Table 1. Sewage sludge had an HHV of 11.88 MJ/kg. The HHV values of the hydrochars increased when compared to raw sludge after performing HTC at a solid-to-liquid ratio of 1:1 at all reaction temperatures. However, the HTC treatment of sewage sludge did not significantly increase energy densification ratio. This could be explained by the transfer of organic components into the liquid phase during HTC, which considerably reduced the HHV (Z. X. Xu et al., 2019). A change in the elemental composition of the solid products was noticed. The HTC of sludge increased the carbon content from 29.75% (sludge) to 33.41% (HTC-1:1–220). Furthermore, the elemental content of O and H in the products decreased dramatically as the reaction temperature increased. For HTC-1:5–220, the O and H content declined by 44.47% and 36.78%, respectively, compared to the sludge feedstock. As shown in Fig. 1, the atomic H/C and O/C ratios were plotted in a Van Krevelen diagram to illustrate the chemical transformation of the organic material to carbon-rich hydrochar. The H/C and O/C atomic ratios of HTC-1:x-220 declined from 1.72 and 0.47 (sludge) to around 1.35–1.41 and 0.12–0.29, respectively. Based on the reaction pathways of sludge to hydrochar via HTC, it was observed that dehydration and carboxylation were involved in the HTC process (Funke and Ziegler,

Table 1
Characteristics of sewage sludge feedstock and hydrochar produced under different conditions at a retention time of 5 h.

Sample	% Yield	Proximate analysis			Ultimate analysis					Atomic ratio		HHV
		VM	Ash	FC	C	H	N	S	O	H/C	O/C	
Sewage sludge		41.86	40.84	17.30	29.75	4.26	5.65	0.69	18.82	1.72	0.47	11.88
HTC-1:1–200	74.10	35.24	48.22	16.54	27.76	3.40	3.99	0.65	15.97	1.47	0.43	11.90
HTC-1:3–200	63.89	34.71	48.78	16.51	30.53	3.64	4.46	0.72	11.87	1.43	0.29	12.81
HTC-1:5–200	54.82	34.51	56.15	9.34	23.16	2.79	3.00	0.83	14.07	1.44	0.46	9.25
HTC-1:7–200	55.63	36.00	58.77	5.23	29.10	3.41	3.77	0.64	4.31	1.41	0.11	11.88
HTC-1:1–210	68.49	33.43	47.79	18.78	31.94	4.08	4.86	0.70	10.63	1.53	0.25	11.42
HTC-1:3–210	57.96	30.45	54.99	14.56	25.43	2.90	3.18	0.89	12.62	1.37	0.37	11.07
HTC-1:5–210	57.27	31.12	53.99	14.89	23.66	2.75	3.00	0.85	15.75	1.39	0.50	9.41
HTC-1:7–210	56.81	29.28	58.59	12.13	28.58	3.46	3.64	0.70	5.03	1.45	0.13	11.44
HTC-1:1–220	62.51	34.52	50.56	14.92	33.41	3.93	4.72	0.72	6.65	1.41	0.15	14.18
HTC-1:3–220	56.23	29.53	59.84	10.63	24.86	2.79	3.18	0.69	8.64	1.35	0.26	10.09
HTC-1:5–220	56.34	32.04	54.91	13.05	23.16	2.73	2.81	0.65	10.45	1.41	0.29	9.40
HTC-1:7–220	53.58	31.75	59.97	8.28	27.89	3.26	3.66	0.82	4.40	1.40	0.12	11.31

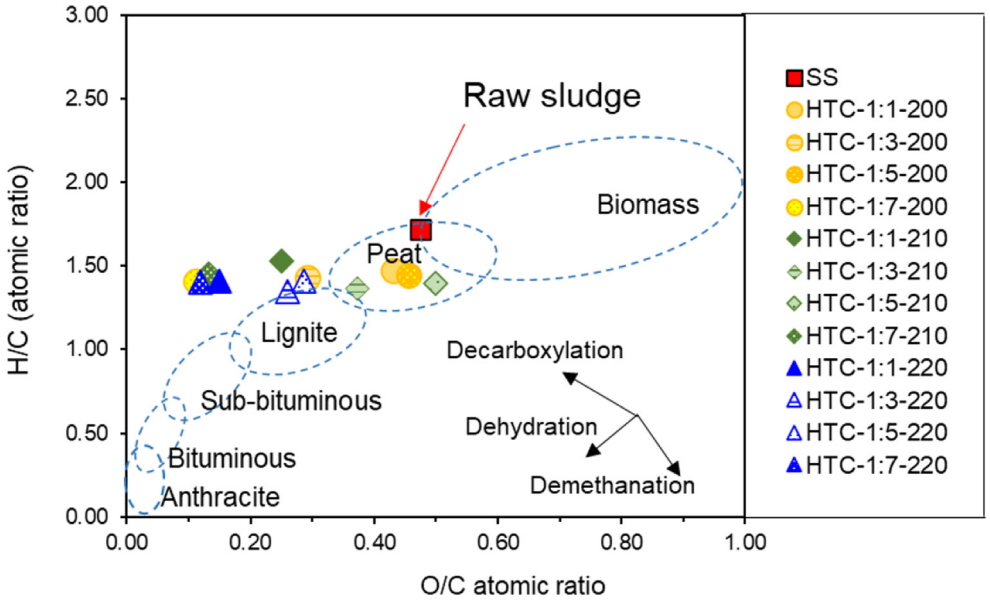

Fig. 1. Van Krevelen diagram of the hydrochars prepared under different conditions.

2010; Smith et al., 2016), while the demethanation reaction was negligible. The H/C and O/C atomic ratios of the solid products were slightly higher than those of the lignite (a low-rank coal) region, with values generally in the range of 0.8–1.3 and 0.2–0.38, respectively (Park and Jang, 2011). Only the HTC-1:5–220 hydrochar was present in the lignite coal region. Therefore, the co-HTC of sludge mixed with other biomass or the co-combustion of blended hydrochars and coal enhanced the combustible properties of hydrochar derived from sludge.

3.2. Fuel properties of hydrochars prepared from co-HTC

The co-HTC treatment of sludge with spent coffee grounds and bagasse was performed to enhance the physicochemical properties of the hydrochar. Table 2 summarizes the proximate analysis of the feedstocks (spent coffee grounds and bagasse) and the hydrochars obtained from co-HTC. HTC-C and HTC-B contained 53.73% and 45.92% VM, respectively, which was significantly higher than the VM content of HTC-S. When sludge and spent coffee grounds were co-hybridized (HTC-SC), a lower proportion of sludge increased the FC and carbon content, while the ash content and hydrochar yield declined (Fig. 2a). The FC content of HTC-S was 13.05%, while the corresponding values of HTC-75%SC, HTC-50%SC, and HTC-25%SC rose to 13.77%, 18.48%, and 26.14%, respectively. The carbon content increased from 27.33% to 55.02% when 25% sludge was mixed with spent coffee grounds (HTC-25%SC). The HHV of the obtained products increased from 9.40 MJ/kg (HTC-S) to 15.62, 18.36, and 22.19 MJ/kg when 75%, 50%, and 25% sludge was supplemented with spent coffee grounds, respectively (Fig. 2c). When the sludge was combined with the agricultural waste bagasse, the fixed carbon content increased to 19.52%, 33.35%, and 42.53% when using 75%, 50%, and 25% sludge by weight, respectively (Fig. 2b). Additionally, the carbon content of HTC-75%SB was 35.32%, while the carbon content of HTC-50%SB and HTC-25%SB rose to 42.42% and 53.79%, respectively. In comparison to HTC-S, the presence of bagasse increased the HHV of hydrochar to 20.33 MJ/kg (HTC-25%SB), as shown in Fig. 2d. Similar trends have been reported previously in the literatures (Zheng et al., 2019; X. Zhang et al., 2017; Ma et al., 2019; Z. X. Xu et al., 2019). To demonstrate the synergistic effect of mixing sludge and biomass, the measured values of the hydrochar properties were compared to the calculated values, as shown in Supplementary Figs. 2 and 3. The calculated value was determined based on an individual raw material, as described in Equation (6). As an illustration of HTC-25%SB, the hydrochar yield was determined by the following calculation:

$$Calculated\ value = 0.25\eta_{s,sludge} + 0.75\eta_{s,bagasse} \quad (6)$$

Table 2
Characteristics of spent coffee grounds and bagasse feedstock as well as hydrochars derived via co-HTC with varying amounts of solid waste over a 5-h retention period.

	Spent coffee grounds	Bagasse	HTC-S (HTC-1:5–220)	HTC-75% SC	HTC-50% SC	HTC-25% SC	HTC-C	HTC-75% SB	HTC-50% SB	HTC-25% SB	HTC-B
Ultimate analysis (wt%)											
C	50.06	41.84	27.33	32.34	44.12	55.02	65.89	35.32	42.42	53.79	63.40
H	7.36	6.25	3.22	4.14	5.22	5.90	6.81	3.95	4.48	4.95	5.20
O	37.97	48.95	10.45	13.84	11.27	10.14	20.54	10.55	18.51	23.47	28.14
N	2.32	0.43	3.44	3.51	3.90	3.91	3.40	3.70	3.41	2.31	0.68
S	0.19	0.16	0.65	0.65	0.37	0.25	0.18	0.50	0.39	0.33	0.08
Proximate analysis											
Volatile matter (%)	74.69	70.98	32.04	40.71	46.39	49.08	53.73	34.49	35.86	42.31	45.92
Fixed carbon (%)	23.21	26.65	13.05	13.77	18.48	26.14	43.08	19.52	33.35	42.53	51.58
Ash (%)	2.10	2.37	54.91	45.52	35.13	24.78	3.19	45.99	30.79	15.16	2.50
Fuel ratio[a]	0.31	0.38	0.41	0.34	0.40	0.53	0.80	0.57	0.93	1.01	1.12
HHV (MJ/kg)	22.31	16.89	9.40	15.62	18.36	22.19	28.24	14.29	17.12	20.33	24.10
Hydrochar yield (%)	N/A	N/A	56.34	64.64	54.42	50.10	40.45	49.94	44.90	42.85	42.75
Energy densification ratio	N/A	N/A	0.79	1.08	1.07	1.13	1.27	1.09	1.19	1.30	1.43

Fuel ratio[a] = Fixed carbon/Volatile matter.
Energy densification ratio = HHV of hydrochar/HHV of feedstock.
Energy Recovery (ER) = (Yield of hydrochar*HHV of hydrochar/HHV of feedstock.

where $\eta_{s,sludge}$ and $\eta_{s,bagasse}$ are hydrochar yields of HTC-S or HTC-B alone. During co-HTC, synergistic effects were observed when a greater proportion of lignocellulosic biomass was added, which increased the relative mass yield of the hydrochars and enhanced their quality.

The fuel ratio was used to evaluate the usefulness of the hydrochars as alternative solid fuels. The results indicated that increasing the fuel ratio by mixing 25 wt% sludge with both spent coffee grounds and bagasse was feasible. The parameter correlated with the HHV of hydrochars and feedstock is energy densification ratio. Energy recovery is defined as the amount of energy that can be recovered relative to the amount of energy stored in the initial substrate (Ipiales et al., 2021). As depicted in Fig. 2e, the energy densification ratio of HTC-SC gradually increased from 0.79 (HTC-S) to 1.13 (HTC-25%SC) as the sludge mixing ratio with spent coffee grounds decreased. HTC-C has the greatest energy densification ratio of 1.27. The energy recovery considerably increased from 44.58% (HTC-S) to 63.2% (HTC-75%SC). After that, energy recovery steadily declined. This was because increasing the amount of sludge increased the percent yield of the hydrochar product. Considering HTC-SB (Fig. 2f), the energy densification ratio continuously increased from 1.09 (HTC-75%SB) to 1.30 (HTC-25%SB) as the sludge ratio decreased. HTC-B had the highest energy densification ratio of 1.43. These results reveal that increasing the amount of lignocellulosic biomass combined with sludge led to an increase in the HHV of the hydrochar. Energy recovery slightly decreased from 47.77% (HTC-75%SB) to 42.74% (HTC-50%SB), then remained relatively stable. In comparison to HTC-S, the co-HTC of sludge with spent coffee grounds and bagasse improved the HHV characteristics, indicating that this material could be used as a solid fuel alternative.

As illustrated in Fig. 3, the H/C and O/C ratios of co-HTC decreased in comparison to the raw materials. The co-HTC process caused the H/C and O/C atomic ratios of HTC-SC and HTC-SB from the biomass stage (feedstocks) to be closer to those of lignite coal. Notably, the hydrochars derived from all sludge mixtures with bagasse were located in the lignite region. In contrast, only HTC-C hydrothermally treated with spent coffee grounds resembled lignite coal. During hydrothermal treatment, co-HTC promoted dehydration and decarboxylation reactions (Smith and Ross, 2016). Low H/C and O/C atomic ratios are considered to be beneficial for solid fuels due to the reduced energy loss and smoke produced during the combustion process (Kambo and Dutta, 2014). Therefore, the addition of spent coffee grounds and bagasse to the sludge significantly improved the HTC product characteristics.

3.3. Migration and transformation behavior of inorganic substances and metals

The inorganic composition of the sludge feedstock and hydrochar produced under the HTC-1:5-220 condition is shown in Supplementary Fig. 4. CaO was the most prevalent compound in the feedstock, followed by SiO_2. After the HTC process, the CaO content decreased and SiO_2 became a major element of the solid product. As illustrated in Fig. 4b, inorganics were extracted from the biomass and leached into the process water during the HTC reaction. High concentrations of Ca and K were observed in the process water, explaining the lower CaO content in the hydrochar. The total heavy metal content in the HTC-S, HTC-50%SC, and HTC-50%SB hydrochars is shown in Fig. 4a. According to the results, the overall heavy metal concentration of the sludge varied substantially, with values in the order of Pb, Cd, Hg, Ni, and As. The leached metal concentrations in the process water of the HTC reaction are displayed in Fig. 4b. This result indicates that all heavy metals were efficiently accumulated in the hydrochars produced using the HTC method (Fig. 4c), which is consistent with Liu et al. (2018). This may be due to the destruction of extracellular matrix components, leading to the dissociation of HMs with weaker bonds (Shi et al., 2013; Wang et al., 2016). In terms of heavy metal leaching toxicity, the highest concentrations of Hg in the process water were found in HTC-S and HTC-50%SC, with concentrations of 0.30 and 0.28 mg/L, respectively. The leached concentrations of all heavy metals (Hg, Pd, Cd, Cd, and As) were lower than the permissible limits established by the industrial wastewater standard of the United States Environmental Protection Agency (EPA) except the Hg concentrations in HTC-S and HTC-50%SC, which was slightly higher than the EPA industrial wastewater standard (Supplementary Table 1).

3.4. Surface properties of raw materials and hydrochars

The FTIR spectra of the raw materials and hydrochars are shown in Fig. 5a, demonstrating the changes in organic functional groups during HTC at various solid-to-liquid ratios. The FTIR spectra of the hydrochars generated under various conditions showed no discernible changes. Compared to raw sludge, the main peaks of the

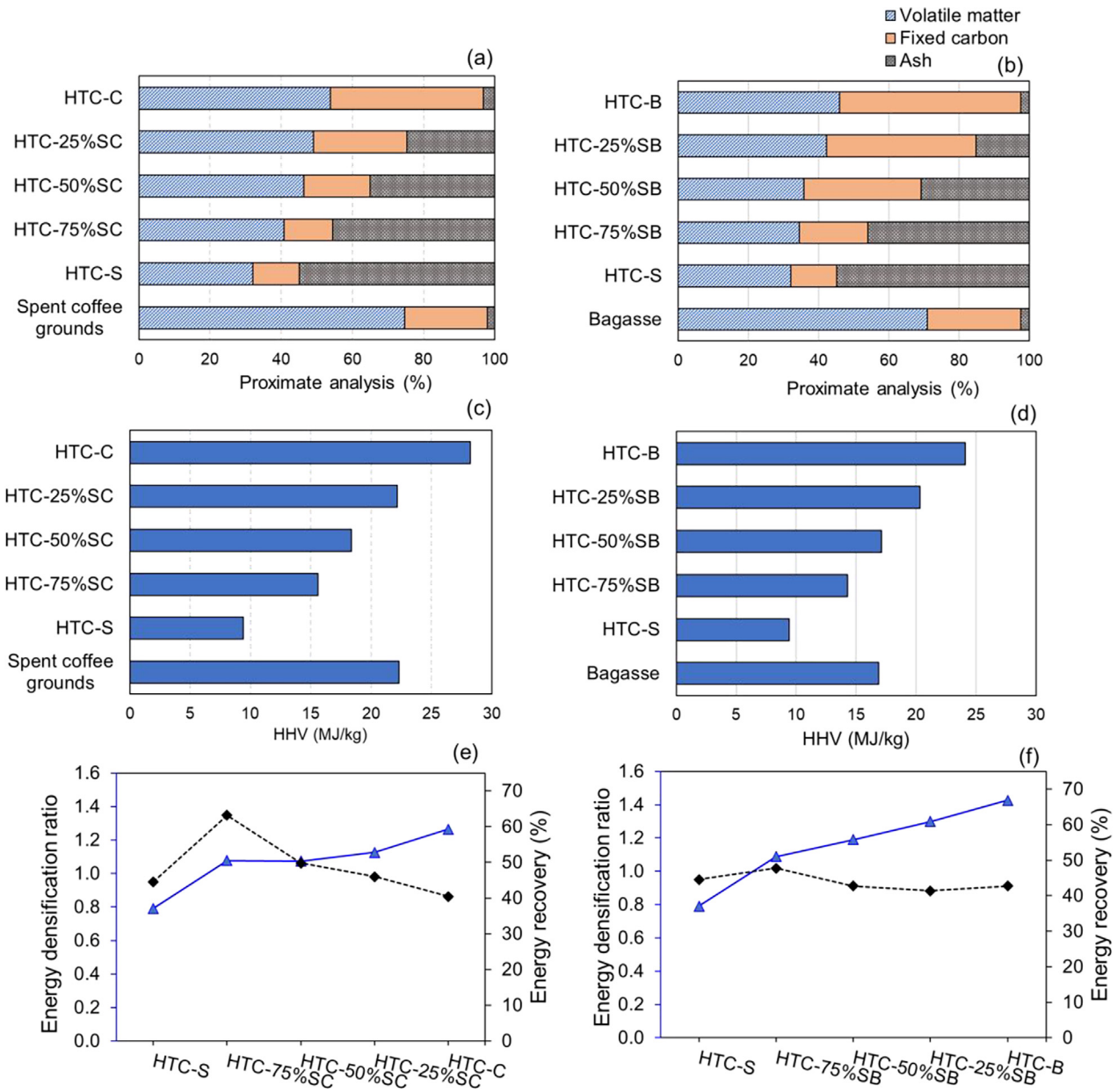

Fig. 2. Hydrochar properties prepared by co-HTC of mixing sludge with spent coffee grounds and bagasse (a) and (b) proximate analysis; (c) and (d) higher heating value; (e) and (f) energy densification ratio and recovery.

hydrochar spectra had stronger intensities, including peaks at 2930 and 2850 cm^{-1} attributed to the stretching vibration of $–CH_2$ (Z. X. Xu et al., 2019), a peak at 1650 cm^{-1} attributed to the stretching vibration of -C = N in amide groups (Zhang et al., 2020), a peak at 1540 cm^{-1} attributed to the asymmetric stretching of -C = O in carboxylic groups (Areeprasert et al., 2014), a peak at 1430 cm^{-1} attributed to $-CH_x$ aliphatic compounds such as $–CH_2$ and $–CH_3$, and a peak at 875 cm^{-1} attributed to $CaCO_3$. The characteristic peak at 1080 cm^{-1} was significantly different in the sludge and hydrochar spectra, and this peak was ascribed to -C-O-R stretching in ethers. This peak indicated that the degree of carbonization was increased, facilitating the formation of OH in the carbonic ring (Z.-X. Xu et al., 2019a). Another possibility for the higher amount of ash produced during HTC is the occurrence of -Si-O stretching.

The FTIR spectra of HTC-SC and HTC-SB are shown in Fig. 5b-c. Between 3600 and 3200 cm^{-1}, a broad band assigned to the –OH vibration in hydroxyl and carboxyl groups was observed in these spectra. This distinctive band was attributed to the cellulose in the spent coffee grounds and bagasse. The FTIR spectrum of HTC-SC showed a peak at 1745 cm^{-1} that was assigned to C = O stretching. This peak was detected with a strong intensity in the spent coffee grounds feedstock spectrum but not the HTC-25%SC and HTC-50%SC spectra. This was due to the decarboxylation reaction and the conversion of some carbon compounds to CO_2 (Kim et al., 2017). The peak at 1580 cm^{-1} may have been formed by alkanes following the HTC reaction (Liu et al., 2017). The peaks at 1160 and 1030 cm^{-1} were detected in the spent coffee grounds feedstock, but they vanished following co-HTC. These peaks were ascribed to C-O-C stretching. After co-HTC treatment, the peak intensities at 2930 and 2850 cm^{-1} assigned to C–H stretching band became weaker. Therefore, structural changes occurred during the hydrothermal reaction. In addition, the higher sludge content in HTC-SC and HTC-SB caused an intense signal at 1080 cm^{-1}, which

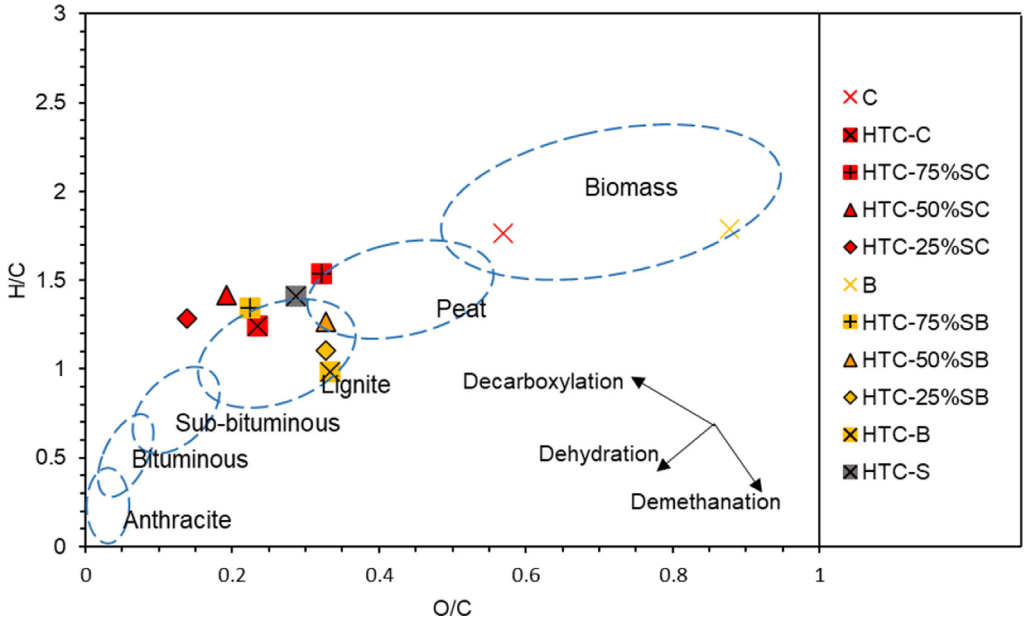

Fig. 3. Van Krevelen diagram of the co-HTC products prepared using sludge, spent coffee grounds, and bagasse.

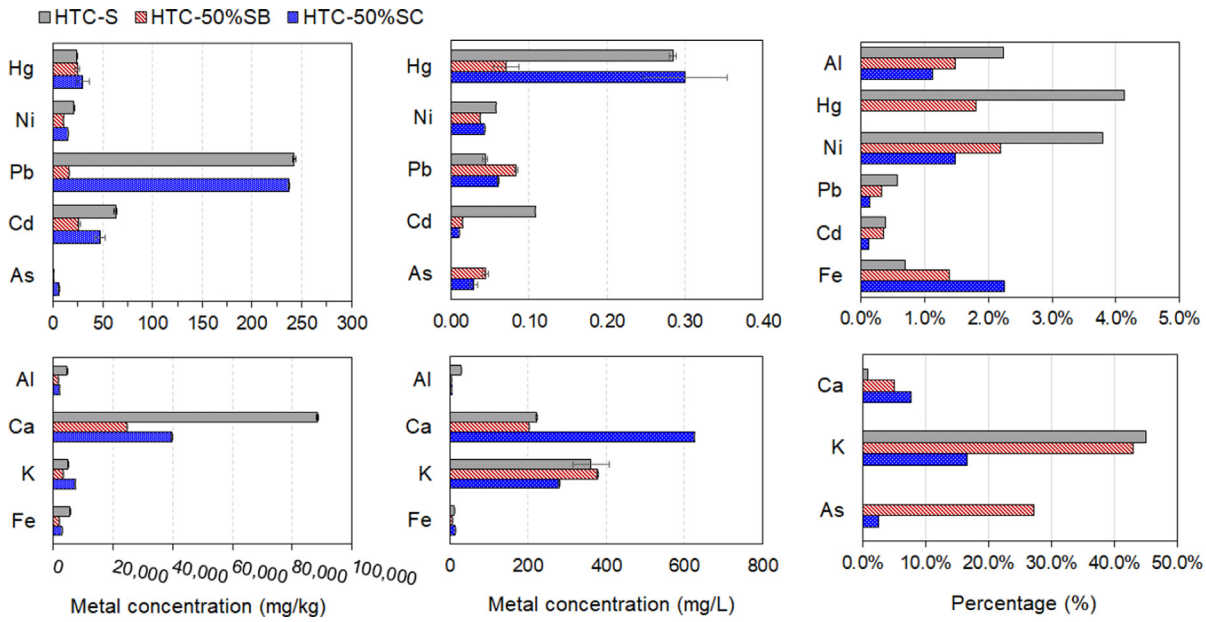

Fig. 4. (a) Metal content in sewage sludge feedstock and hydrochars; (b) leached metal concentration in process water; (c) percentage of metal in process water determined by ICP-OES.

was ascribed to the Si-O-Si vibrations obtained from sludge. The spent coffee grounds and bagasse ash content (Table 2) show that the feedstock contained a small amount of ash, so there was no absorption peak at this location. As shown in Fig. 5c, a peak at 1720 cm^{-1} was identified as C = O (J. Zhang et al., 2017). In the FTIR spectra of HTC-B and HTC-75%SB, this peak was more intense than that of the bagasse feedstock spectrum. Following the HTC reaction, the peak at 1580 cm^{-1} was more intense in the HTC-B and HTC-75%SB spectra. This peak was caused by alkanes generated during the HTC reaction (Liu et al., 2017). The peak at 1240 cm^{-1} was assigned to C-O-C stretching. This peak was found in the feedstock spectra but not the HTC product spectra. This was due to the deoxygenation reactions of the biomass during HTC (Melo et al., 2017). The peak at 1030 cm^{-1}, indicating the C–O bond of primary hydroxyl, was observed in the bagasse feedstock spectrum. The intensity of this peak declined after co-HTC because the C–O bond was likely broken due to decarboxylation reactions (Kim et al., 2017). The absorption peak at 1455 cm^{-1} corresponded to aromatic C = C stretching. This peak became more prominent following HTC, indicating a greater degree of carbonization in the samples. This indicates that aromatization (dehydrogenation, demethanation, and decarbonylation) increases the intensity of all solid products (Song et al., 2019; Z. X. Xu et al., 2019). In conclusion, HTC is suitable for removing volatile aliphatic substances, oxygen functional groups, and minerals.

SEM images of the as-synthesized hydrochars prepared from sludge and sludge blended with spent coffee grounds and bagasse are shown in Fig. 6. The sludge feedstock had a non-uniform parti-

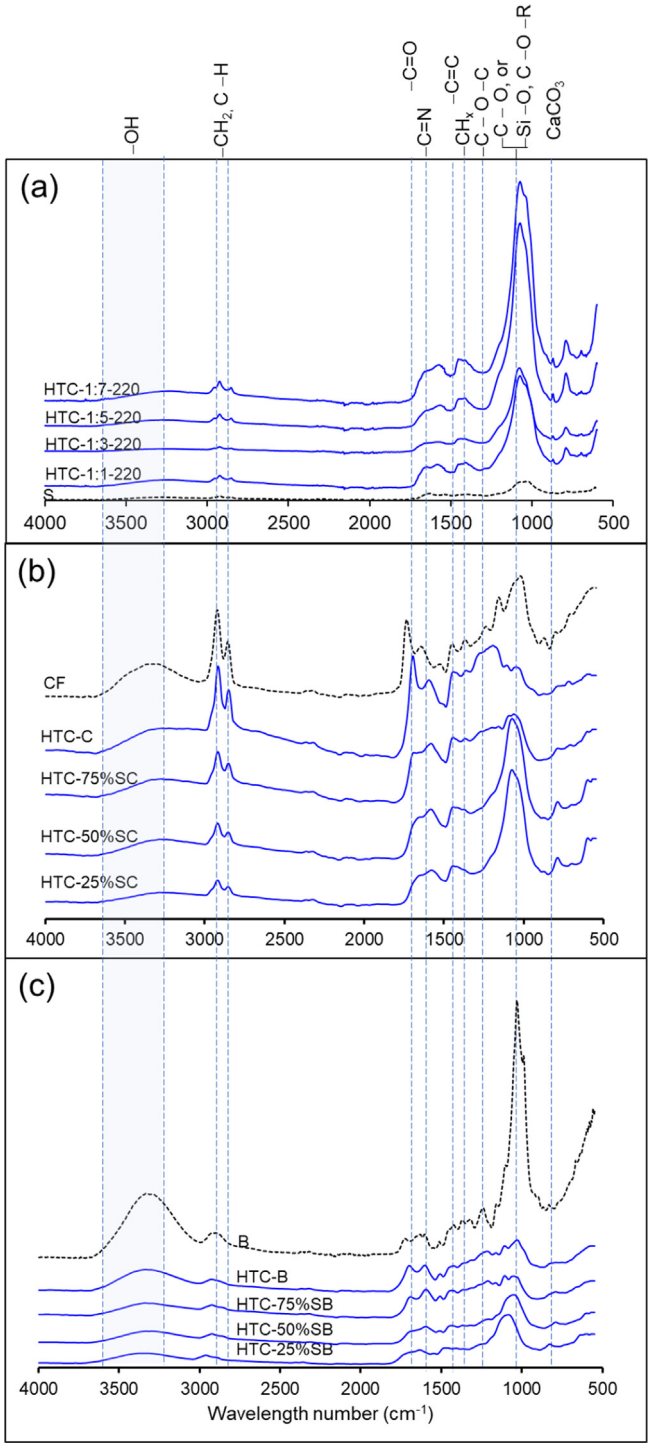

Fig. 5. FTIR spectra of (a) HTC-S, (b) HTC-SC, and (c) HTC-SB.

cle size ranging from 49.0 to 67.5 μm. The morphology of the sludge considerably changed after HTC, transforming into a porous structure via dehydration and decarboxylation reactions with a particle size of around 4.78–20.50 μm (Fig. 6b) (He et al., 2013). The HTC-50%SC and HTC-50%SB samples had a spherical shape (Fig. 6c and d). This result was in good agreement with Xu et al. (2018), who reported hydrochar products with a spherical morphology derived from the HTC of hydroxypropyl methyl cellulose. The carbon microspheres were generated by the polymerization of products formed via the hydrolysis of lignocellulosic materials (Sevilla and Fuertes, 2009; Wu et al., 2016).

3.5. Combustion behavior and thermal characteristics of as-synthesized products

TGA-DTG characterization was carried out to investigate the combustion properties of the feedstock and hydrochars. The TGA and DTG curves of sludge, HTC-S, HTC-50%SC, and HTC-50%SB are shown in Fig. 7. The DTG curves revealed four stages in the decomposition of these solid materials in an air atmosphere, including a dehydration stage, devolatilization and combustion stage, char combustion stage, and thermal decomposition of minerals and other inorganic compounds stage (Li et al., 2020). The temperatures associated with these stages are shown in Table 3. For the sludge feedstock, significant weight loss was observed in the devolatilization and combustion of volatile matter stage (230–330 °C) due to the high VM content of the sludge. Compared to char combustion, devolatilization of biomass typically occurs at relatively lower temperatures (Xu and Sheng, 2012). 26.3% weight loss was achieved at this stage, which was significantly higher than the 16.2% weight loss experienced by HTC-S (Fig. 7b). This was because some micromolecular volatile matter was dissolved during HTC (Supplementary Fig. 1), resulting in lower VM content in the hydrochar product. After HTC treatment, the hydrochar did not significantly change in the transition period between the devolatilization and combustion stage and the char combustion stage. This was because the hydrochar had low FC content. The compensatory impact of FC and VM caused the VM and char combustion stages of the co-HTC products to become distinct. FC increased from 13.05% for HTC-S to 18.48% and 33.35% for HTC-50%SC and HTC-50%SB, respectively. This result was comparable to that of hydrothermally treated sewage sludge reported by He et al. (2013), in which an increase in FC content was associated with an intense peak in the DTG char stage. The weight loss rate of a mixture of biomass with sludge was greater than that of HTC-S, indicating that a larger amount of fixed carbon is generated during the combustion of char stage (He et al., 2019). Normally, the increasing amount of oxidative carbon during the char combustion stage can yield a high content of fixed carbon, resulting in a high degree of thermal stability (Lu et al., 2020).

Table 3 displays the characteristic temperatures of the temperatures. The ignition temperature (T_i) is an essential factor for minimizing fire and explosion risk. When using hydrochar as a fuel, T_i slightly increased relative to sludge (from 237 to 255 °C) after hydrothermal treatment. As shown in Table 2, the hydrochar had lower VM content after treatment, resulting in a higher ignition temperature. This implied a higher difficulty of ignition. However, T_i did not exceed 20 °C. This was potentially due to the high ash content of the hydrochar (HTC-S), especially Ca and K (Fig. 4a), which can have a substantial catalytic influence on combustion reactivity. Xu and Sheng (2012) investigated the effect of inorganic matter in solid fuel products and found that Ca and K had a significant catalytic effect on devolatilization. The ignition temperatures of the HTC-50%SC and HTC-50%SB samples increased to 263 and 288 °C, respectively. This was due to the lower ash in hydrochars had a significant catalytic effect on the combustion reactivity (He et al., 2019; Kanti et al., 2020; Kanti et al., 2021). A high T_i indicated a lower fire and explosion risk (He et al., 2013). Therefore, the hydrochar derived from the co-HTC of spent coffee grounds and bagasse with sludge had improved efficacy in terms of safe handling, storage, and transport. However, the combustibility index S of HTC-50%SC and HTC-50%SB was less than that of sludge. A lower *T*i contributed to the higher S index of sludge. This indicated that co-HTC hydrochar burned less violently, which contributed to its stable combustion in the furnace (Li et al., 2020). Moreover, the

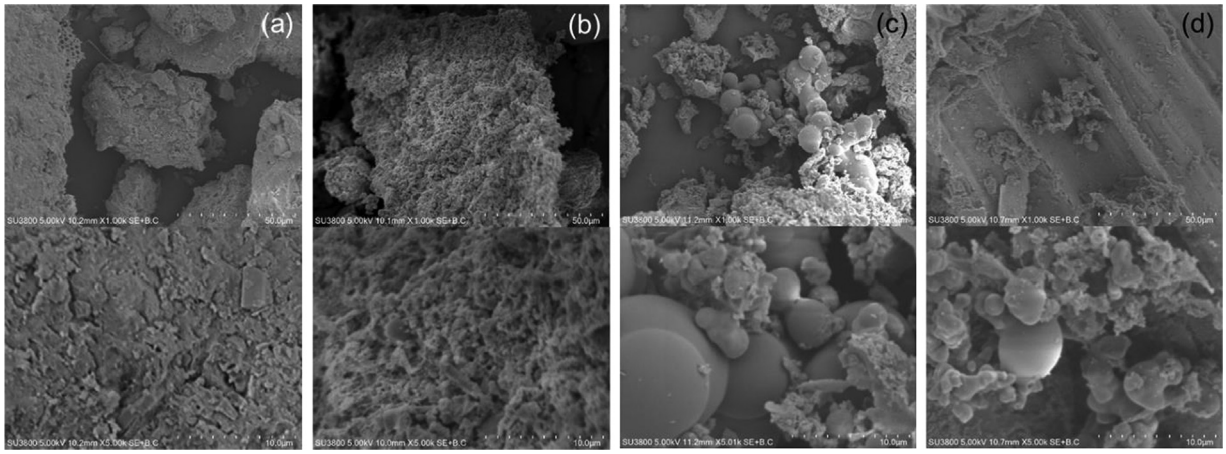

Fig. 6. SEM images at 1.0 k and 5.0 k of (a) sludge, (b) HTC-S, (c) HTC-50%SC, and (d) HTC-50%SB.

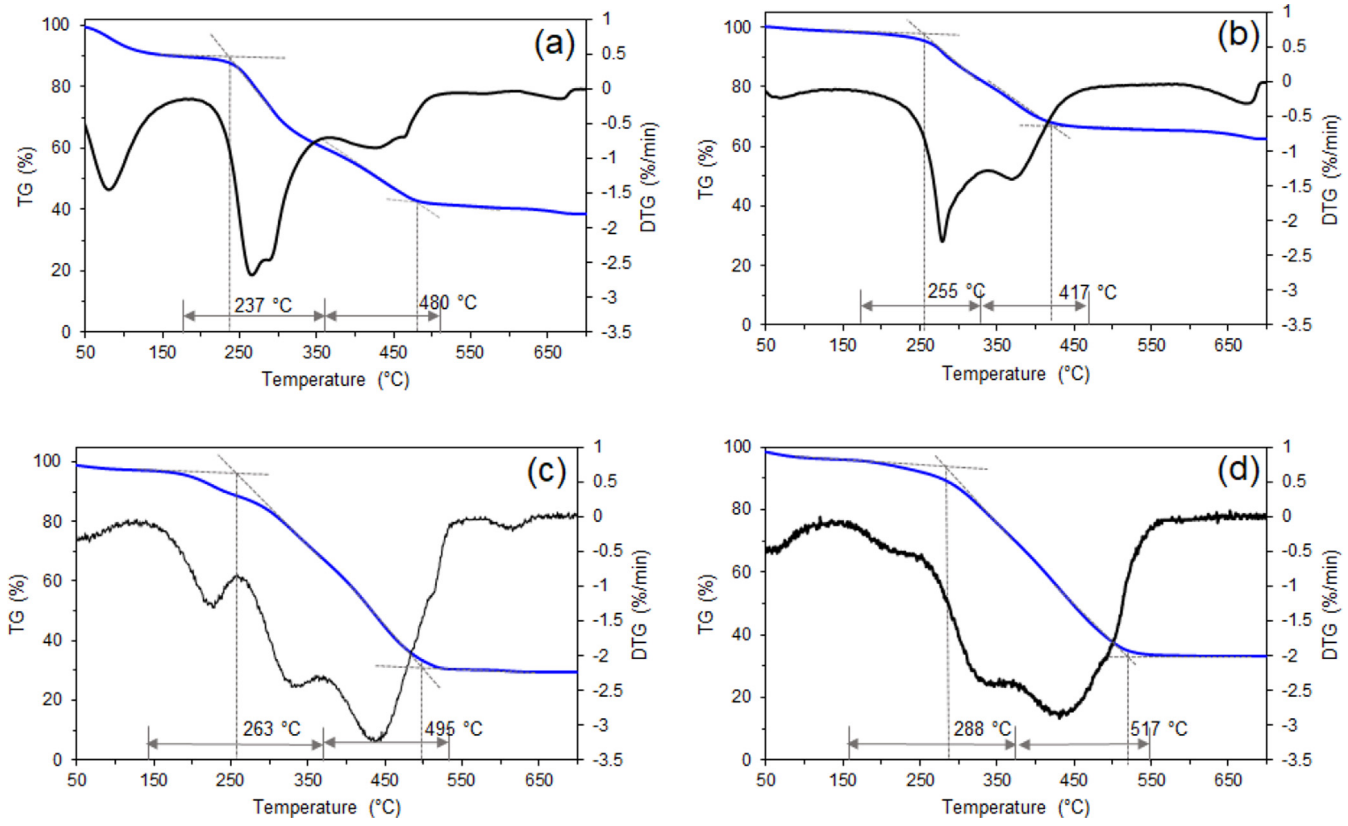

Fig. 7. Thermal analysis (TGA/DTG) of (a) raw sewage sludge and the obtained hydrochars: (b) HTC-S, (c) HTC-50%SC, and (d) HTC-50%SB.

T_b and T_{max} values increased after co-HTC, implying that the combination of lignocellulosic biomass resulted in hydrochars with a more stable chemical structure and greater thermostability. In conclusion, the combustion behavior of the hydrochar obtained from sludge was unsatisfactory. However, performing co-HTC using sludge blended with lignocellulosic biomass can feasibly address the shortcomings of the sludge-only hydrochar. At any mixing ratio, a relatively low level of ash and a high level of fixed carbon were achieved.

The co-combustion behavior of commercial coal blended with various proportions of HTC-S was studied, as shown in Fig. 8 and Table 3. The commercial coal had a high amount of fixed carbon, requiring greater activation energy. Adding HTC-S to coal lowered the ignition temperature from 501 °C (coal) to 258 °C (50%HTC-S/coal). This was caused by the higher content of high-volatile compounds in the HTC-S (Muthuraman et al., 2010). Additionally, the addition of hydrochar increased the S index. 10%HTC-S/coal exhibited the highest S index (Li et al., 2020).

3.6. Combustion kinetics analysis

The activation energy (E) and pre-exponential factor (A) were calculated using the Coat & Redfern model, as reported in Equation (5). These parameters are regarded as the two most important kinetic parameters for the combustion reaction analysis of sludge and hydrochars. Using linear regression based on the Coat & Red-

Table 3
Combustion parameters of raw sludge, bio-coal, hydrochars, and hydrochar-biocoal co-combustion.

	Devolatilization and combustion-stage D	Char combustion-stage C	Characteristic temperatures					S index*10^8
			T_i (°C)	T_m (°C)	T_b (°C)	DTG_{max}	DTG_{mean}	
Sludge	230–330	330–430	237	266	480	−2.68	−0.49	4.9
HTC-S	220–320	345–450	255	374	417	−2.40	−0.57	5.0
HTC-50%SC	165–360	380–535	263	437	495	−75.0	−0.02	5.3
HTC-50%SB	250–350	375–550	288	432	517	−63.0	−0.02	3.2
Coal	–	445–648	431	634	646	−44.60	−1.38	51.4
10%HTC-S/coal	–	464–630	293	600	626	−41.50	−1.29	102.0
30%HTC-S/coal	251–443	443–650	290	573	640	−32.73	−1.15	68.7
50%HTC-S/coal	239–457	457–656	285	630	630	−27.93	−0.95	50.6

T_i = ignition temperature.
T_b = burnout temperature.
T_m = temperature at maximum mass loss rate.
DTG_{max} = maximum mass loss rate.
DTG_{mean} = mean combustion rate.

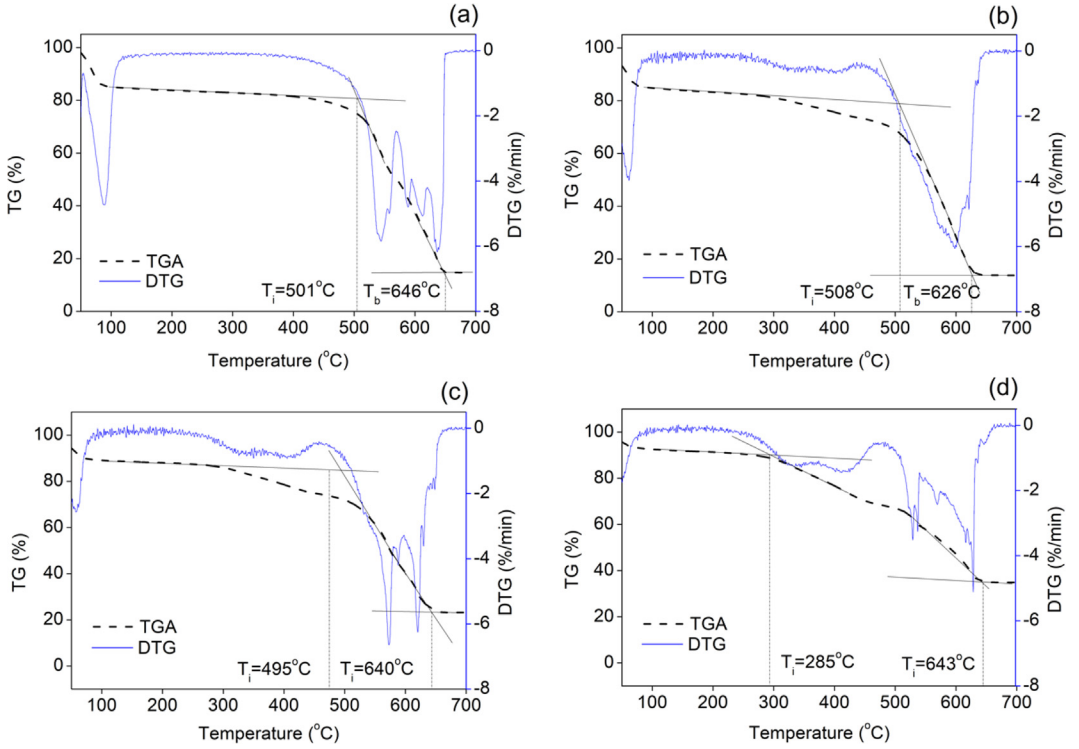

Fig. 8. TGA and DTG curves of the co-combustion of (a) coal, (b) 10% HTC-S/coal, (c) 30% HTC-S/coal, and (d) 50% HTC-S/coal blends.

Table 4
Activation energies of solid products.

	Activation energy (kJ/mol)					
	VM stage	R^2	A	Char stage	R^2	A
S	31.82	0.99	75.61	10.44	0.96	7.40
HTC-S	43.97	0.97	599.31	31.19	0.96	44.16
HTC-50%SC	20.11	0.99	2.81	38.04	0.99	163.25
HTC-50%SB	10.90	0.98	0.28	42.20	0.99	183.47

fern equation, data from various combustion stages were used to determine the kinetic parameters. According to Table 4, the E and A values of HTC-50%SC and HTC-50%SB during the devolatilization combustion stage were relatively low compared to those of raw sludge and HTC-S. The E and A values of HTC-50%SC were 20.11 kJ/mol and 2.81, while those of HTC-50%SB were 10.90 kJ/mol and 0.28, respectively. This implies that the co-HTC products may be more combustible than HTC-S, which is consistent with their VM content. For the char combustion stage, the sludge feedstock had the lowest E and A values of 10.44 kJ/mol and 7.40, respectively. This was potentially due to the lower concentration of fixed carbon (Peng et al., 2016). The E values of the co-HTC products in the char stage (38.04 kJ/mol for HTC-50 % SC and 42.20 kJ/mol for HTC-50 % SB) were greater than that of HTC-S. Meanwhile, the A values for the char stage rose from 44.16 (HTC-S) to 163.25 (HTC-50%SC) and 183.47 (HTC-50%SB). This demonstrates that

Table 5
Activation energies of the co-combustion of coal blended with HTC-S.

	Activation energy (kJ/mol)					
	VM stage	R^2	A	Char stage	R^2	A
Coal	N/A	N/A	N/A	138.18	0.91	1.97×10^8
10%HTC-S/coal	N/A	N/A	N/A	157.84	0.95	3.87×10^9
30%HTC-S/coal	8.81	0.99	0.12	108.95	0.96	2.07×10^6
50%HTC-S/coal	2.66	0.99	0.03	462.48	0.96	7.13×10^{30}

the combustion of hydrochars derived through co-HTC is expected to exhibit greater stability and longevity compared to the combustion of hydrochars produced individually. It can be attributed to the decomposition of VM and the improved conversion of VM into FC during the co-HTC process (He et al., 2019).

The E and A values of commercial coal blended with HTC-S were also analyzed. The activation energy values corresponding to the stages of volatile and char combustion weight loss are summarized in Table 5. Weight loss occurred in a single char combustion stage during the combustion of coal. The low VM content of 10%HTC-S/coal meant that the activation energy was not able to be calculated during the VM stage. The reactivity of the 10%HTC-S blended with coal was found to be comparable to that of coal. This outcome was consistent with the results of Muthuraman et al. (2010). For 30% and 50%HTC-S/coal, two distinct regions were observed. The E values in the VM stage of 30% and 50%-HTC-S were significantly different from that of HTC-S, indicating that HTC-S interacted with coal during combustion. However, the E value of 50%HTC-coal in the char stage was much higher compared to that of coal. This indicates the limitations of blending hydrochar with coal in an excess proportion.

This work demonstrates that the hydrochars derived from co-HTC exhibited stable and durable combustion in comparison to the hydrochar derived from individual sludge materials. The higher E values of the char stage of the co-HTC hydrochars were greater than that of HTC-S, indicating that the fixed carbon in the co-HTC products was more stable (Zheng et al., 2019). The co-combustion behavior of hydrothermally treated sludge blended with commercial coal demonstrates that an appropriate mixing ratio (30%HTC-S blend) improves the devolatilization properties of coal. The ignition temperature gradually decreases with increasing HTC-S content. Therefore, the volatile matter removed from hydrothermally treated sludge is burned, releasing sufficient energy to lower the ignition temperature of the coal.

4. Conclusion

A facile co-hydrothermal carbonization of metal oxide-rich sewage sludge and spent coffee grounds or bagasse was proposed as a sustainable method to produce biocoal-like solid fuel. The addition of spent coffee grounds and bagasse could enhance the fuel properties of the solid products, remarkably increasing fixed carbon content, combustion reactivity, and high heating value (HHV) along with a low ash content. Moreover, the co-combustion of hydrochar and coal could also improve the devolatilization properties and ignition of coal. This strategy indicated that co-HTC sewage sludge combined with spent coffee grounds or bagasse is highly suitable for producing an alternative solid fuel. It is a prospective approach to increase the value-added of sewage sludge feedstock for bicoal production in the future.

CRediT authorship contribution statement

Siridet Piboonudomkarn: Formal analysis. **Pongtanawat Khemthong:** Formal analysis, Validation, Visualization. **Saran Youngjan:** Formal analysis. **Kitirote Wantala:** Formal analysis, Validation. **Visanu Tanboonchuy:** Formal analysis. **Yingyote Lubphoo:** . **Rattabal Khunphonoi:** Conceptualization, Formal analysis, Visualization, Supervision.

Declaration of Competing Interest

The authors declare that they have no known competing financial interests or personal relationships that could have appeared to influence the work reported in this paper.

Acknowledgments

This work was financially supported by Office of the Permanent Secretary, Ministry of Higher Education, Science, Research and Innovation (Grant no. RGNS 64-049), the French Ministry of Europe and Foreign Affairs (MEAE), the French Ministry of Higher Education, Research and Innovation (MESRI) and the MHESI, the Research Center for Environmental and Hazardous Substance Management (EHSM), Khon Kaen University, and the Faculty of Engineering, Khon Kaen University. This work was conducted under the research on Enhanced technology and circular-biomaterial utilization for environmental abatement by the Faculty of Engineering, Khon Kaen University, which has received funding support from the Fundamental Fund (the National Science, Research and Innovation Fund (NSRF), Thailand). The authors would also like to acknowledge the National Nanotechnology Center (NANOTEC) and the Program Management Unit for Human Resources & Institutional Development, Research and Innovation (Grant no. B40G660031).

Appendix A. Supplementary material

Supplementary data to this article can be found online at https://doi.org/10.1016/j.arabjc.2023.105315.

References

Areeprasert, C., Zhao, P., Ma, D., Shen, Y., Yoshikawa, K., 2014. Alternative solid fuel production from paper sludge employing hydrothermal treatment. Energy & Fuels 28, 1198–1206. https://doi.org/10.1021/ef402371h.

Bardhan, M., Novera, T.M., Tabassum, M., Islam, M.d., Azharul, I., Atikul, M.d., Hameed, B.H., 2021. Co-hydrothermal carbonization of different feedstocks to hydrochar as potential energy for the future world: A review. J. Clean. Prod. 298,. https://doi.org/10.1016/j.jclepro.2021.126734 126734.

Coimbra, R.N., Paniagua, S., Escapa, C., Calvo, L.F., Otero, M., 2016. Thermal valorization of pulp mill sludge by co-processing with coal. Waste Biomass Valorization 7, 995–1006. https://doi.org/10.1007/S12649-016-9524-2/TABLES/3.

Cong, K., Han, F., Zhang, Y., Li, Q., 2019. The investigation of co-combustion characteristics of tobacco stalk and low rank coal using a macro-TGA. Fuel 237, 126–132. https://doi.org/10.1016/J.FUEL.2018.09.149.

Danso-Boateng, E., Shama, G., Wheatley, A.D., Martin, S.J., Holdich, R.G., 2015. Hydrothermal carbonisation of sewage sludge: Effect of process conditions on product characteristics and methane production. Bioresour. Technol. 177, 318–327. https://doi.org/10.1016/j.biortech.2014.11.096.

Funke, A., Ziegler, F., 2010. Hydrothermal carbonization of biomass: A summary and discussion of chemical mechanisms for process engineering. Biofuels, Bioprod. Bioref. 4, 160–177. https://doi.org/10.1002/bbb.198.

Gai, C., Chen, M., Liu, T., Peng, N., Liu, Z., 2016. Gasification characteristics of hydrochar and pyrochar derived from sewage sludge. Energy 113, 957–965. https://doi.org/10.1016/j.energy.2016.07.129.
Hansen, L.J., Fendt, S., Spliethoff, H., 2022. Impact of hydrothermal carbonization on combustion properties of residual biomass. Biomass Convers. Biorefin. 12, 2541–2552. https://doi.org/10.1007/s13399-020-00777-z.
He, C., Giannis, A., Wang, J.-Y., 2013. Conversion of sewage sludge to clean solid fuel using hydrothermal carbonization: Hydrochar fuel characteristics and combustion behavior. Appl. Energy 111, 257–266. https://doi.org/10.1016/j.apenergy.2013.04.084.
He, C., Zhang, Z., Ge, C., Liu, W., Tang, Y., Zhuang, X., Qiu, R., 2019. Synergistic effect of hydrothermal co-carbonization of sewage sludge with fruit and agricultural wastes on hydrochar fuel quality and combustion behavior. Waste Manage. 100, 171–181. https://doi.org/10.1016/J.WASMAN.2019.09.018.
Ipiales, R.P., de la Rubia, M.A., Diaz, E., Mohedano, A.F., Rodriguez, J.J., 2021. Integration of hydrothermal carbonization and anaerobic digestion for energy recovery of biomass waste: An overview. Energy & Fuels 35, 17032–17050. https://doi.org/10.1021/acs.energyfuels.1c01681.
Kambo, H.S., Dutta, A., 2014. Strength, storage, and combustion characteristics of densified lignocellulosic biomass produced via torrefaction and hydrothermal carbonization. Appl. Energy 135, 182–191. https://doi.org/10.1016/j.apenergy.2014.08.094.
Kanti, P., Sharma, K.V., Ramachandra, C.G., Azmi, W.H., 2020. Experimental determination of thermophysical properties of Indonesian fly-ash nanofluid for heat transfer applications. Part. Sci. Technol 39, 597–606 https://doi.org/10.1080/02726351.2020.1806971.
Kanti, P.K., Sharma, K.V., Said, Z., Gupta, M., 2021. Experimental investigation on thermo-hydraulic performance of water-based fly ash–Cu hybrid nanofluid flow in a pipe at various inlet fluid temperatures. Int. Commun. Heat Mass Transfer 124,. https://doi.org/10.1016/J.ICHEATMASSTRANSFER.2021.105238 105238.
Khoo, C.G., Lam, M.K., Mohamed, A.R., Lee, K.T., 2020. Hydrochar production from high-ash low-lipid microalgal biomass via hydrothermal carbonization: Effects of operational parameters and products characterization. Environ. Res. 188,. https://doi.org/10.1016/j.envres.2020.109828 109828.
Kim, D., Lee, K., Bae, D., Park, K.Y., 2017. Characterizations of biochar from hydrothermal carbonization of exhausted coffee residue. J. Mater. Cycles Waste Manag. 19, 1036–1043. https://doi.org/10.1007/s10163-016-0572-2.
Koottatep, T., Fakkaew, K., Tajai, N., Pradeep, S.V., Polprasert, C., 2016. Sludge stabilization and energy recovery by hydrothermal carbonization process. Renew. Energy 99, 978–985. https://doi.org/10.1016/j.renene.2016.07.068.
Li, Y., Liu, H., Xiao, K., Jin, M., Xiao, H., Yao, H., 2020. Combustion and pyrolysis characteristics of hydrochar prepared by hydrothermal carbonization of typical food waste: Influence of carbohydrates, proteins, and lipids. Energy & Fuels 34, 430–439. https://doi.org/10.1021/acs.energyfuels.9b02940.
Lin, Y., Ma, X., Peng, X., Hu, S., Yu, Z., Fang, S., 2015. Effect of hydrothermal carbonization temperature on combustion behavior of hydrochar fuel from paper sludge. Appl. Therm. Eng. 91, 574–582. https://doi.org/10.1016/j.applthermaleng.2015.08.064.
Liu, M., Duan, Y., Bikane, K., Zhao, L., 2018. The migration and transformation of heavy metals in sewage sludge during hydrothermal carbonization combined with combustion. Biomed. Res. Int. 2018, 1–11. https://doi.org/10.1155/2018/1913848.
Liu, C., Huang, X., Kong, L., 2017. Efficient low temperature hydrothermal carbonization of Chinese Reed for biochar with high energy density. Energies (Basel) 10, 2094. https://doi.org/10.3390/en10122094.
Lu, X., Ma, X., Chen, X., Yao, Z., Zhang, C., 2020. Co-hydrothermal carbonization of polyvinyl chloride and corncob for clean solid fuel production. Bioresour. Technol. 301,. https://doi.org/10.1016/J.BIORTECH.2020.122763 122763.
Lu, X., Ma, X., Chen, X., 2021. Co-hydrothermal carbonization of sewage sludge and lignocellulosic biomass: Fuel properties and heavy metal transformation behaviour of hydrochars. Energy 221,. https://doi.org/10.1016/j.energy.2021.119896 119896.
Ma, J., Chen, M., Yang, T., Liu, Z., Jiao, W., Li, D., Gai, C., 2019. Gasification performance of the hydrochar derived from co-hydrothermal carbonization of sewage sludge and sawdust. Energy 173, 732–739. https://doi.org/10.1016/j.energy.2019.02.103.
Martinez-Hernandez, E., Amezcua-Allieri, M.A., Sadhukhan, J., Anell, J.A., 2018. Sugarcane bagasse valorization strategies for bioethanol and energy production, in: Sugarcane - technology and research. InTech. https://doi.org/10.5772/intechopen.72237.
Massaya, J., Pickens, G., Mills-Lamptey, B., Chuck, C.J., 2021. Enhanced hydrothermal carbonization of spent coffee grounds for the efficient production of solid fuel with lower nitrogen content. Energy & Fuels 35, 9462–9473. https://doi.org/10.1021/acs.energyfuels.1c00870.
McNutt, J., He, Q. (Sophia), 2019. Spent coffee grounds: A review on current utilization. Journal of Industrial and Engineering Chemistry 71, 78–88. https://doi.org/10.1016/j.jiec.2018.11.054.
Melo, C.A., Junior, F.H.S., Bisinoti, M.C., Moreira, A.B., Ferreira, O.P., 2017. Transforming sugarcane bagasse and vinasse wastes into hydrochar in the presence of phosphoric acid: An evaluation of nutrient contents and structural properties. Waste Biomass Valorization 8, 1139–1151. https://doi.org/10.1007/s12649-016-9664-4.
Mumme, J., Titirici, M.-M., Pfeiffer, A., Lüder, U., Reza, M.T., Mašek, O., 2015. Hydrothermal carbonization of digestate in the presence of zeolite: Process efficiency and composite properties. ACS Sustain. Chem. Eng. 3, 2967–2974. https://doi.org/10.1021/acssuschemeng.5b00943.
Muthuraman, M., Namioka, T., Yoshikawa, K., 2010. Characteristics of co-combustion and kinetic study on hydrothermally treated municipal solid waste with different rank coals: A thermogravimetric analysis. Appl. Energy 87, 141–148. https://doi.org/10.1016/j.apenergy.2009.08.004.
Nanda, S., Gong, M., Hunter, H.N., Dalai, A.K., Gökalp, I., Kozinski, J.A., 2017. An assessment of pinecone gasification in subcritical, near-critical and supercritical water. Fuel Process. Technol. 168, 84–96. https://doi.org/10.1016/j.fuproc.2017.08.017.
Olajire, A.A., 2020. The brewing industry and environmental challenges. J. Clean. Prod. 256,. https://doi.org/10.1016/J.JCLEPRO.2012.03.003 102817.
Paiboonudomkarn, S., Wantala, K., Lubphoo, Y., Khunphonoi, R., 2023. Conversion of sewage sludge from industrial wastewater treatment to solid fuel through hydrothermal carbonization process. Mater. Today Proc. 75, 85–90. https://doi.org/10.1016/J.MATPR.2022.11.107.
Park, S.-W., Jang, C.-H., 2011. Characteristics of carbonized sludge for co-combustion in pulverized coal power plants. Waste Manage. 31, 523–529. https://doi.org/10.1016/j.wasman.2010.10.009.
Peng, C., Zhai, Y., Zhu, Y., Xu, B., Wang, T., Li, C., Zeng, G., 2016. Production of char from sewage sludge employing hydrothermal carbonization: Char properties, combustion behavior and thermal characteristics. Fuel 176, 110–118. https://doi.org/10.1016/j.fuel.2016.02.068.
Peng, C., Zhai, Y., Hornung, A., Li, C., Zeng, G., Zhu, Y., 2018. Promoting effect of ZSM-5 catalyst on carbonization via hydrothermal conversion of sewage sludge. ACS Sustain. Chem. Eng. 6, 9461–9469. https://doi.org/10.1021/acssuschemeng.8b02012.
Reza, M.T., Yang, X., Coronella, C.J., Lin, H., Hathwaik, U., Shintani, D., Neupane, B.P., Miller, G.C., 2016. Hydrothermal carbonization (HTC) and pelletization of two arid land plants bagasse for energy densification. ACS Sustain. Chem. Eng. 4, 1106–1114. https://doi.org/10.1021/acssuschemeng.5b01176.
Saberian, M., Li, J., Donnoli, A., Bonderenko, E., Oliva, P., Gill, B., Lockrey, S., Siddique, R., 2021. Recycling of spent coffee grounds in construction materials: A review. J. Clean. Prod. 289,. https://doi.org/10.1016/j.jclepro.2021.125837 125837.
Sattasathuchana, S., Parnthong, J., Youngian, S., Faungnawakij, K., Rangsunvigit, P., Kitiyanan, B., Khunphonoi, R., Wanichsombat, A., Grisdanurak, N., Khemthong, P., 2023. Energy efficiency of bio-coal derived from hydrothermal carbonized biomass: Assessment as sustainable solid fuel for municipal biopower plant. Appl. Therm. Eng. 221,. https://doi.org/10.1016/j.applthermaleng.2022.119789 119789.
Sevilla, M., Fuertes, A.B., 2009. Chemical and structural properties of carbonaceous products obtained by hydrothermal carbonization of saccharides. Chem. - Eur. J. 15, 4195–4203. https://doi.org/10.1002/chem.200802097.
Shi, W., Liu, C., Ding, D., Lei, Z., Yang, Y., Feng, C., Zhang, Z., 2013. Immobilization of heavy metals in sewage sludge by using subcritical water technology. Bioresour. Technol. 137, 18–24. https://doi.org/10.1016/j.biortech.2013.03.106.
Smith, A.M., Ross, A.B., 2016. Production of bio-coal, bio-methane and fertilizer from seaweed via hydrothermal carbonisation. Algal Res. 16, 1–11. https://doi.org/10.1016/j.algal.2016.02.026.
Smith, A.M., Singh, S., Ross, A.B., 2016. Fate of inorganic material during hydrothermal carbonisation of biomass: Influence of feedstock on combustion behaviour of hydrochar. Fuel 169, 135–145. https://doi.org/10.1016/j.fuel.2015.12.006.
Song, Y., Zhan, H., Zhuang, X., Yin, X., Wu, C., 2019. Synergistic characteristics and capabilities of co-hydrothermal carbonization of sewage sludge/lignite mixtures. Energy & Fuels 33, 8735–8745. https://doi.org/10.1021/acs.energyfuels.9b01766.
Tasca, A.L., Puccini, M., Gori, R., Corsi, I., Galletti, A.M.R., Vitolo, S., 2019. Hydrothermal carbonization of sewage sludge: A critical analysis of process severity, hydrochar properties and environmental implications. Waste Manage. 93, 1–13. https://doi.org/10.1016/j.wasman.2019.05.027.
Tong, W., Liu, Q., Ran, G., Liu, L., Ren, S., Chen, L., Jiang, L., 2019. Experiment and expectation: Co-combustion behavior of anthracite and biomass char. Bioresour. Technol. 280, 412–420. https://doi.org/10.1016/J.BIORTECH.2019.02.055.
Wang, X., Li, C., Zhang, B., Lin, J., Chi, Q., Wang, Y., 2016. Migration and risk assessment of heavy metals in sewage sludge during hydrothermal treatment combined with pyrolysis. Bioresour. Technol. 221, 560–567. https://doi.org/10.1016/j.biortech.2016.09.069.
Wang, R., Wang, C., Zhao, Z., Jia, J., Jin, Q., 2019. Energy recovery from high-ash municipal sewage sludge by hydrothermal carbonization: Fuel characteristics of biosolid products. Energy 186,. https://doi.org/10.1016/j.energy.2019.07.178 115848.
Wang, C., Zhang, X., Liu, Y., Che, D., 2012. Pyrolysis and combustion characteristics of coals in oxyfuel combustion. Appl. Energy 97, 264–273. https://doi.org/10.1016/j.apenergy.2012.02.011.
Wu, L.M., Tong, D.S., Li, C.S., Ji, S.F., Lin, C.X., Yang, H.M., Zhong, Z.K., Xu, C.Y., Yu, W. H., Zhou, C.H., 2016. Insight into formation of montmorillonite-hydrochar nanocomposite under hydrothermal conditions. Appl. Clay Sci. 119, 116–125. https://doi.org/10.1016/j.clay.2015.06.015.
Xu, Z.-X., Cheng, J.-H., He, Z.-X., Wang, Q., Shao, Y.-W., Hu, X., 2019a. Hydrothermal liquefaction of cellulose in ammonia/water. Bioresour. Technol. 278, 311–317. https://doi.org/10.1016/j.biortech.2019.01.061.
Xu, M., Sheng, C., 2012. Influences of the heat-treatment temperature and inorganic matter on combustion characteristics of cornstalk biochars. Energy & Fuels 26, 209–218. https://doi.org/10.1021/ef2011657.
Xu, Z.X., Song, H., Zhang, S., Tong, S.Q., He, Z.X., Wang, Q., Li, B., Hu, X., 2019. Co-hydrothermal carbonization of digested sewage sludge and cow dung biogas

residue: Investigation of the reaction characteristics. Energy 187,. https://doi.org/10.1016/J.ENERGY.2019.115972 115972.
Xu, Z.-X., Song, H., Li, P.-J., He, Z.-X., Wang, Q., Wang, K., Duan, P.-G., 2020. Hydrothermal carbonization of sewage sludge: Effect of aqueous phase recycling. Chem. Eng. J. 387,. https://doi.org/10.1016/j.cej.2019.123410 123410.
Xu, Y., Xia, M., Jiang, Y., Li, F., Xue, B., 2018. Opal promotes hydrothermal carbonization of hydroxypropyl methyl cellulose and formation of carbon nanospheres. RSC Adv. 8, 20095–20107. https://doi.org/10.1039/C8RA01138A.
Yang, G., Zhang, G., Wang, H., 2015. Current state of sludge production, management, treatment and disposal in China. Water Res. 78, 60–73. https://doi.org/10.1016/j.watres.2015.04.002.
Zhai, Y., Peng, C., Xu, B., Wang, T., Li, C., Zeng, G., Zhu, Y., 2017. Hydrothermal carbonisation of sewage sludge for char production with different waste biomass: Effects of reaction temperature and energy recycling. Energy 127, 167–174. https://doi.org/10.1016/j.energy.2017.03.116.
Zhang, J., Gao, J., Chen, Y., Hao, X., Jin, X., 2017. Characterization, preparation, and reaction mechanism of hemp stem based activated carbon. Results Phys. 7, 1628–1633. https://doi.org/10.1016/j.rinp.2017.04.028.
Zhang, S., Pi, M., Su, Y., Xu, D., Xiong, Y., Zhang, H., 2020. Physiochemical properties and pyrolysis behavior evaluations of hydrochar from co-hydrothermal treatment of rice straw and sewage sludge. Biomass Bioenergy 140,. https://doi.org/10.1016/j.biombioe.2020.105664 105664.
Zhang, X., Zhang, L., Li, A., 2017. Hydrothermal co-carbonization of sewage sludge and pinewood sawdust for nutrient-rich hydrochar production: Synergistic effects and products characterization. J. Environ. Manage. 201, 52–62. https://doi.org/10.1016/J.JENVMAN.2017.06.018.
Zheng, C., Ma, X., Yao, Z., Chen, X., 2019. The properties and combustion behaviors of hydrochars derived from co-hydrothermal carbonization of sewage sludge and food waste. Bioresour. Technol. 285,. https://doi.org/10.1016/j.biortech.2019.121347 121347.